9-26-2012

Resolution Enhancement Optimizations for Hyperspectral and Multispectral Synthetic Image Fusion

Charles R. Bostater

Resolution Enhancement Optimizations for Hyperspectral and Multispectral Synthetic Image Fusion

Charles R. Bostater

Marine Environmental Optics Laboratory and Remote Sensing Center, College of Engineering, Florida Institute of Technology, 150 West University Blvd., Melbourne, Florida, USA 32901

ABSTRACT

Many sensor systems are available for sensing the earth surface from satellites as well as airborne and mobile platforms. Thus, fusing data from multiple sensors is becoming a common theme in earth remote sensing. A major goal of remote sensing image fusion is resolution enhancement. In this paper, optimization techniques are presented and discussed in order to help make an image fusion process a practical method for not only spectral signature based image analysis but also for algorithm development in remote sensing of water. The technique described and explored in this paper includes the identification of feature areas, stratified random pixel selection, singular value decomposition model building for synthetic image generation, and optimization of the 2D Butterworth filter cutoff and order coefficients in a spectral and spatial resolution enhancement protocol. The process is also called spatial sharpening of hyperspectral imagery as presented in this paper. Examples of methods for estimating errors in the data fusion process are also described using coastal littoral zone remote sensing imagery with an emphasis on weathered oil scenes. The optimization and testing of a data fusion methodology or protocol described utilizes image to image georeferencing methods, nearest neighborhood and linear remapping of multi-resolution spatial and spectral imagery. The central optimization procedures entails random selection of pixels from feature areas in simultaneously acquired multispectral and hyperspectral scenes in order to build multiple "SVD" singular value decomposition models and optimized selection of these image models for each hyperspectral channel based upon the non-parametric K-S p-statistical test. The model synthetic imagery is then used with the 2D discrete cosine and inverse cosine filters, a 2D Butterworth filter. Optimization of the 2D Butterworth filter cutoff and order coefficients are conducted for each hyperspectral band and these coefficients are optimized using the same K-S based tests. The above optimization protocol results in synthetic reflectance hyperspectral cube where minimization between observed and synthetic hyperspectral signatures has been performed for each hyperspectral channel. Results indicate the synthetic hyperspectral resolution enhancement methodology is most sensitive to (a) the pixels selected (from feature areas) for use in the SVD model building process and (b) the 2D Butterworth cutoff frequency selected.

Keywords: image fusion, target detection, feature detection, ocean sensing, littoral zones, airborne sensors, airborne, hyperspectral, multispectral, subsurface imaging, cameras, oil spills, data fusion, 2D Butterworth filter, resolution enhancement, image sharpening, spectral sharpening, spatial sharpening.

INTRODUCTION

Background

A data fusion technique utilizes information derived from multiple sensing systems in order to derive new types of data or bio-geophysical variables as suggested in Figure 1. An example, in physical oceanography is the calculation of the density of seawater. To properly make this measurement a seawater temperature sensor, conductivity sensor and pressure sensor is used to calculate the density. The data from the sensors are “fused using a mathematical algorithm” call an equation of state. In remote sensing of the water surface and subsurface features, multi sensor outputs can be combined for estimating bio-geochemical and physical variables. Imaging sensors commonly used in remote sensing however have different radiometric, temporal, spatial and spectral resolution. These need to be accounted for in fusing imaging data derived from multiple imaging systems. The application described in this paper is an implementation of a data fusion technique commonly referred to as spectral spatial sharpening – a form of image resolution enhancement[1,2,3].

*Corresponding author cbostate@fit.edu. [1]College of Engineering, Florida Institute of Technology, 150 West University Blvd., Melbourne, Fl, USA; 321-258-9134.

Remote Sensing of the Ocean, Sea Ice, Coastal Waters, and Large Water Regions 2012, edited by Charles R. Bostater Jr., Stelios P. Mertikas, Xavier Neyt, Caroline Nichol, Dave C. Cowley, Jean-Paul Bruyant, Proc. of SPIE Vol. 8532, 85320E

The purpose of the optimized data fusion technique described in this paper is to (1) increase the spatial resolution in one imaging sensor's channels by utilizing an overlapping set of pixels of another sensor's pixels – each sensor providing different spatial and spectral resolution and (2) to increase the spectral resolution (in terms of number of bands or channels) in order to increase not only the spatial resolution but also to increase the number of channels. This resolution enhancement or spectral-spatial sharpening is depicted in Figure 1. The methodology as well as the art of the techniques described improves upon previously described techniques[2, 3, 4, 5] by including "*optimization procedures and methods*". These have been found to be required in order to improve the "*synthetic*" spectral signatures obtained in the spectral-spatial sharpening process or resolution enhancement[4] data fusion approach. Without the optimizations described, the utility of the enhanced spectral resolution is limited for applied remote sensing.

The schematic shown in Figure 1 represents the overall process where the low spatial resolution (x, y) HSI image with many channels (λ) is *mathematically* combined with a multispectral (MS) image of the same geographical coverage but with fewer spectral channels in order to "sharpen" the spatial domain and provide spectral signatures for the smaller spatial pixels. The optimized resolution enhancement protocol yields "synthetic HS image cubes" [6,7].

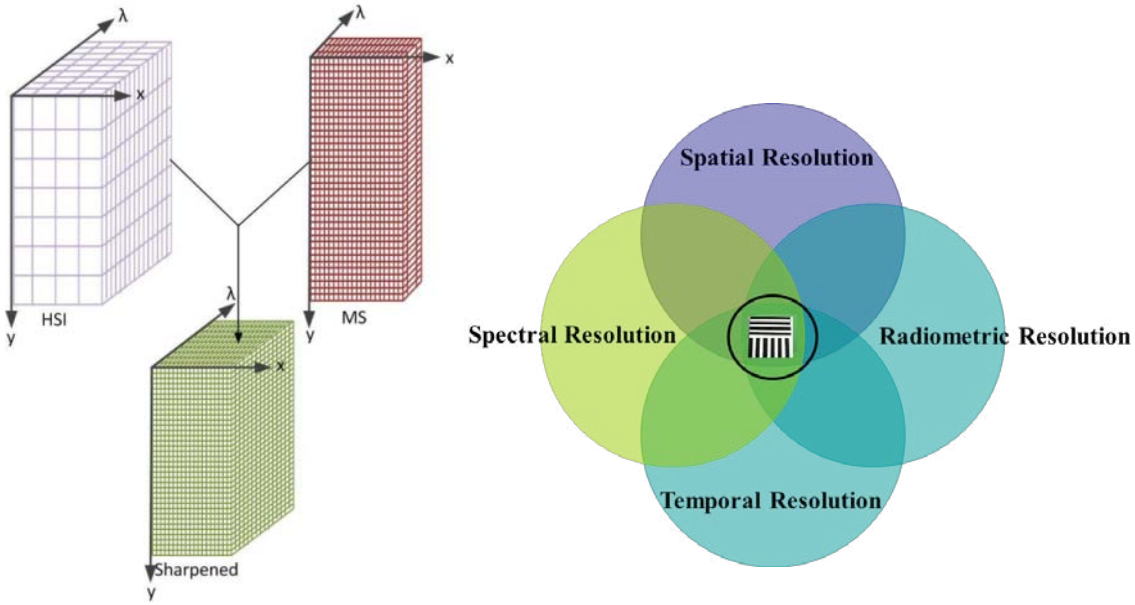

Figure 1. Upper left schematic: a high-spectral but low-spatial-resolution (HSI) hyperspectral image (the front face represent the image pixel spatial-resolution and the depth represent the number of bands and spectral resolution). The MS image: a high-spatial but low-spectral-resolution (only 3 bands in depth) image. Both images are mathematical fused in order to form a resulting high-spectral and high-spatial resolution "enhanced" synthetic hyperspectral cube of atmospherically corrected bidirectional reflectance. A Euler diagram schematic (right) used to explain that resolution enhancement methodologies or remote sensing image fusion can be considered as development of mathematical relations between the elemental sets of the resolutions used in remote sensing science in order to increase the resolution of any 2 or more intersecting resolutions. The goal is to enhance the information content within an intersecting set in order to increase scientific understanding of a feature within a scene – such as a target or feature anomaly within an image. An example is using spatial and spectral overlap between imagery to create new information concerning feature and target anomalies.

The societal value of this research involves improving the spatial resolution and spectral resolution of satellite, airborne, mobile or fixed platform imagery for use in environmental surveillance and monitoring in order to enhance situational awareness and knowledge by using material signatures. Outputs from the methodology or optimized protocol[6] can assist in land, water or littoral zone management and other decision making where spectral–spatial image anomalies need to be scientifically understood. The imagery utilized in this paper to demonstrate the optimization results were acquired as part of a data acquisition program using airborne flights following the Deepwater Horizon (DWH) oil and gas release in the Northern Gulf of Mexico in 2010. Flight and vessel data collected during February, March, and April 2011, in the Northern Gulf of Mexico - along the Florida Panhandle, coastal islands south of Alabama, Mississippi, and in Barataria Bay, Louisiana have been utilized to demonstrate the optimized resolution enhancement methodology. Additional data along the eastern coastal waters in Florida in the

Banana River Lagoon, collected during April and May 2011 have also been used to help test the efficacy of the optimized data fusion techniques[6,7].

It is important to realize that the mathematical methods reported on below, are not the "image fusion" process commonly considered today in geographical information (GIS) and related image processing where data layers or imagery are essentially overlaid, perhaps using "*layer transparency techniques*" as shown in Figure 2.

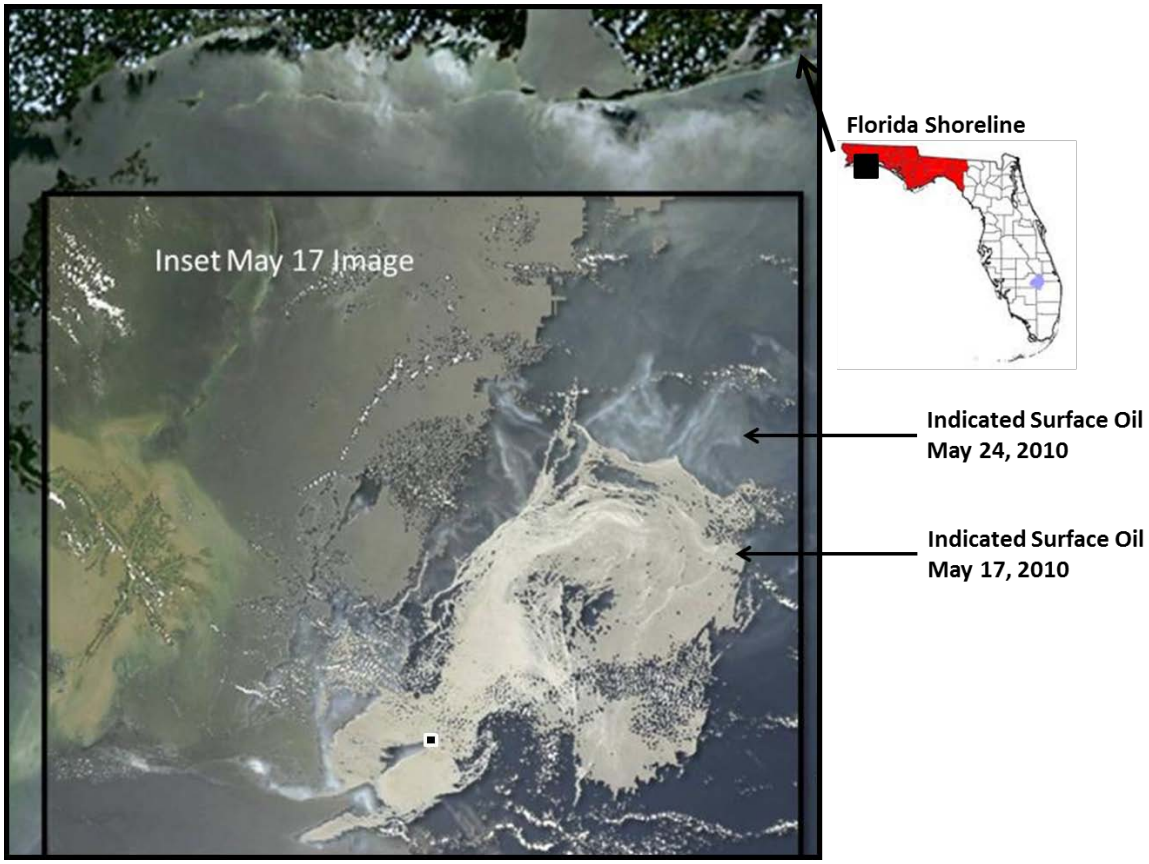

Figure 2. Example of a simple image layer GIS transparency technique using imagery acquired by satellite during the Deepwater Horizon oil and gas spill. A NASA MODIS image on May 17, 2010 is overlaid on the May 24, 2010 MODIS false color image using a GIS layer "transparency" technique. The technique allowed for the estimation of the dispersion and net surface movement of the oil sheen moving towards the Florida Panhandle at a spatial rate of over 3 km/day. The technique is not considered a resolution enhancement or image fusion technique since data or imagery is only overlaid – not mathematically fused as described below.

The multispectral (MS) and hyperspectral imagery (HSI) used in this paper have high spatial and spectral resolution compared to many systems available today. The hyperspectral imagery with $\leq$ 0.5 m pixel size are fused with imagery acquired simultaneously using a large frame aerial camera with scanned 9 inch color negative film with $\leq$ 10 cm pixel sizes. Data collected from a small vessel[7] has MS spatial scales of ~5mm and the hyperspectral imagery collected from the vessel has a spatial scale of $\leq$ 5 cm. The MS imagery presented below has 3 spectral channels and the HSI system collects 64-1024 spectral channels. Improvements to the data fusion process involves the (1) selection of pixels to be used in singular value decomposition (SVD) using "feature areas", (2) optimal SVD model coefficient selection, and (3) optimization of parameters used in a two dimensional (2-D) Butterworth filter by (3) minimizing the difference between observed, modeled and synthetic spectral signatures using nonparametric K-S statistical p-statistic tests. The sensing systems utilized are known to provide useful information in environmental surveillance and monitoring of land and water features, oil feature detection, species discrimination, bottom feature detection and vegetation dysfunction assessments[6, 7, 8, 9] as well as for environmental quality or environmental security issues[9]. Additional imagery information is available at http://www.bostater.info.

2. TECHNIQUES & METHODS

2.1 Imaging Systems and Imagery used in the Image Fusion Methodology

The image fusion examples reported in this paper utilizes imagery acquired from a hyperspectral imaging (HSI) system described below and imagery simultaneously taken from a photogrammetric 9 inch film camera. The color negative film images are scanned to produce ~255 megapixel digital images with high spatial resolution. Mapping camera imagery used in the resolution enhancement mathematical methodology was collected over littoral zones at ~1,225 m altitude between 10 AM local time to 4 PM local during March, 2011, with a 12 inch focal plane lens, 1/225 second shutter speed and aperture adjusted for optimal contrast and exposure of the photogrammetric negative film. The large format (9 in^2) color negatives were scanned at 2400 dpi using scanners with special glass plates (Scanatron) that minimize the presence of "newton rings" in each 3 band image. High speed AGFA X400PE1 color negative aerial film was used. The aerial negative scanning process is calibrated using a scanned target with known sub-millimeter scales 0.005 mm to 5 um resolution and follows NIST traceable standards. The process results in three band multispectral images with spectral response curves published by the film manufacturer. *In-situ* laboratory and field targets are typically used for spatial calibration of the MS imagery using a combination of white, black or gray scale targets. These targets are used for calibrating the spatial pixel sizes obtained in the film to digital conversion process and are used for spatial resolution assessments, image enhancements, DGPS geo-referencing and ground control point location. A MS image mosaic georeferenced flight line along Florida's panhandle is shown in Figure 3 and is used in the spectral –spatial resolution enhancement described in this paper.

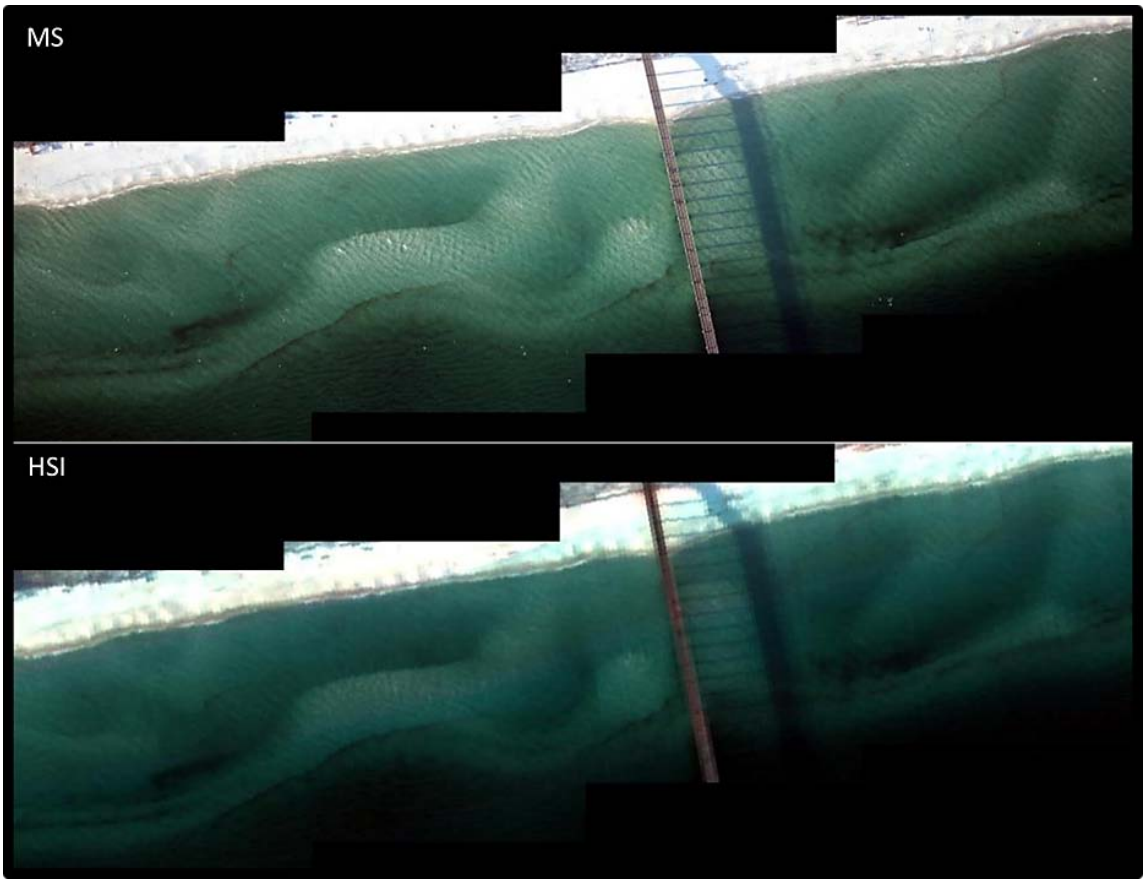

Figure 3. Mosaic of registered and rectified scanned multispectral (MS) imagery (top) and simultaneously collected hyperspectral (HS) imagery (bottom) used to perform spectral-spatial resolution enhancement. Imagery was collected March 12, 2011 along the Florida coastal waters in the Northern Gulf of Mexico at Navarre Beach Pier, 30o22'33.68"N 86051'46.76"W collected March 12, 2011 at 4,00 feet, westbound PM flight line.

The detail in the MS scanned digital imagery allows for high resolution “spatial resolution enhancement” with the overlapping set of high spectral resolution HS imagery as shown in Figure 3. Figure 4 shows the spatial detail available in the fusion process from the photogrammetric scanned imagery. The yellow outlined area in the HS image is shows the same sub-region in Figure 5, used in a resolution enhancement and result shown in the results.

Figure 4. A MS littoral zone image along the Florida Panhandle. The image indicates submerged “weathered” oil in the littoral zone shallow waters. This image and a subset of the above HS cube shown below above are georeferenced and rectified using an image to image registration process before the mathematical SVD model building process and filtering process is applied.

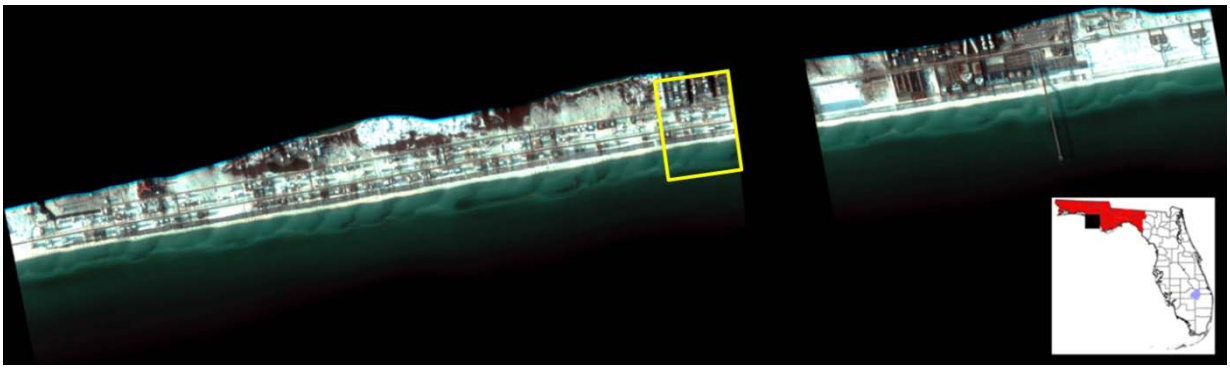

Figure 5. Northern Gulf of Mexico, Florida Panhandle hyperspectral (HS) atmospherically corrected[10,11] reflectance image flight line RGB image (488, 530, 684) collected March 12, 2011 westbound at 4,000 ft altitude at Navarre Beach Pier (30°22'33.37"N 86°51'46.88"W) west of Destin Florida and the entrance to Choctawhatchee Bay. The yellow sub-region in this HSI image is the same area shown as Figure 4.

The HSI system used to acquire the littoral zone imagery shown in Figures 3,5 and 7 are used in the optimized image fusion process. The HS imaging system (built by the author) is gimbal mounted in order to maintain a relatively constant orientation of the camera by using the downward gravitational force vector. A strapped down inertial motion unit (IMU) mounted at the camera provides information in order to correct the pushbroom sensor imagery

for platform yaw, pitch and roll using the approach depicted in the control systems diagram[12] in Figures 6. Platform directional changes are also included in the pushbroom image correction processing methodology using DGPS (5 HZ updates) data along with the IMU (60 HZ). The average altitude above MSL during the acquisition of the HSI and MS imagery used in this paper was approximately 4106 ft. or 1251.5 m. The integration time or exposure time was ~3 to 4 ms and yielded pixel dimensions (ground sampling area) of ~ 0.644 m by ~ 0.332 m. The spectral resolution (FWHH) is ~3.77 nm based upon calibration using spectral line sources. All imagery was collected under clear sky conditions, calm wind conditions, with flight lines in the plane of the sun's movement. The hyperspectral imaging system is capable of collecting 64 to 1024 channels and a swath of spatial 1376 pixels, and calibrated 39 degree field of view (FOV) lens.

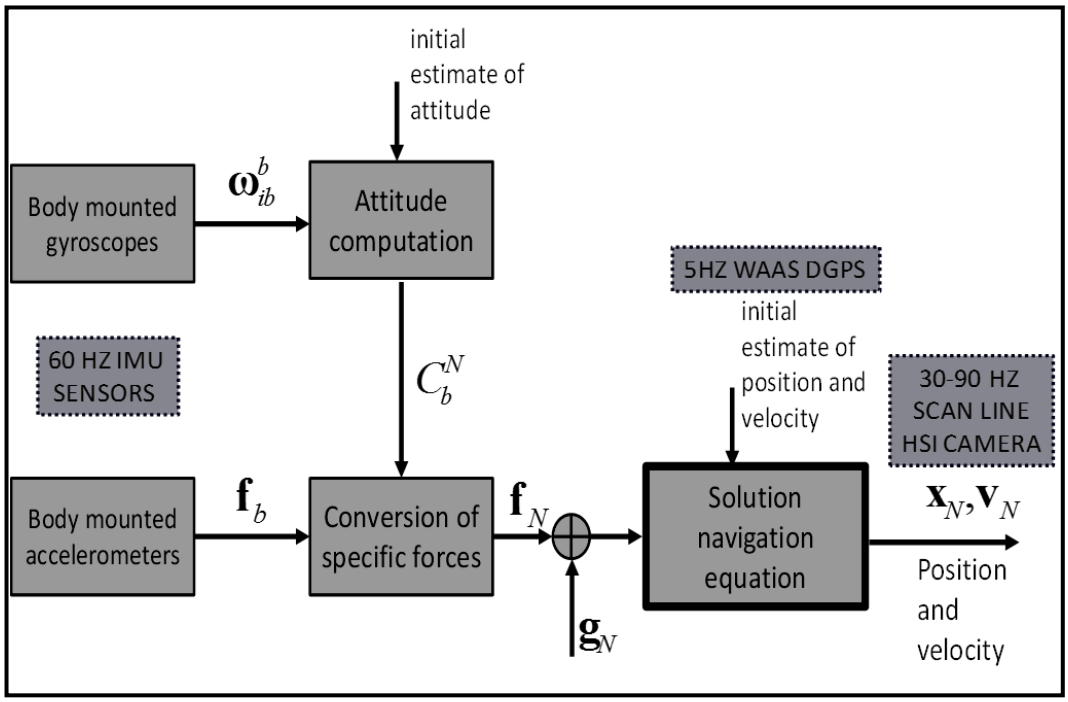

Figure 6. A control system schematic indicating sensor inputs, data rates and computations used in the Kalman based control system post processing used to solve for the position of the center of a HSI pushbroom scan line on the earth's surface. Resampling of the DGPS and IMU sensor data is applied to match the HSI pushbroom camera data rate. The control system algorithms were developed in the Marine and Environmental Optics Laboratory (modified after Bostater, et al.[12]).

The HSI system is calibrated for radiance using dual Optronic Laboratories 18 inch calibration spheres (traceable to NIST standards) and standard spectral line sources for wavelength calibration across the 1024 spectral channels of the 2D CCD camera. Atmospherically corrected reflectance images taken on March 12, 2011 are shown in Figure 3, 5 and 7. Experience suggests the above system provides necessary information in order to prepare the pushbroom sensor imagery for resolution enhancement protocol applications.

Multisensor[13] *simultaneously* collected imagery is needed to conduct the spectral-spatial resolution enhancements described in the next section. As can be seen in Figure 8, the littoral zone subsurface features change dramatically over time due to high wave energy typical along shorelines and coastal surf zone areas. Figure 8 suggests the change in indicated subsurface weathered oil along the Florida Panhandle from the period fall 2010 to spring 2011. Without simultaneously collected multisensory imagery, the "spectral" quality of the resulting image fusion protocol methodology can be a factor producing a *blurring effect* in the resulting enhanced synthetic hyperspectral cube.

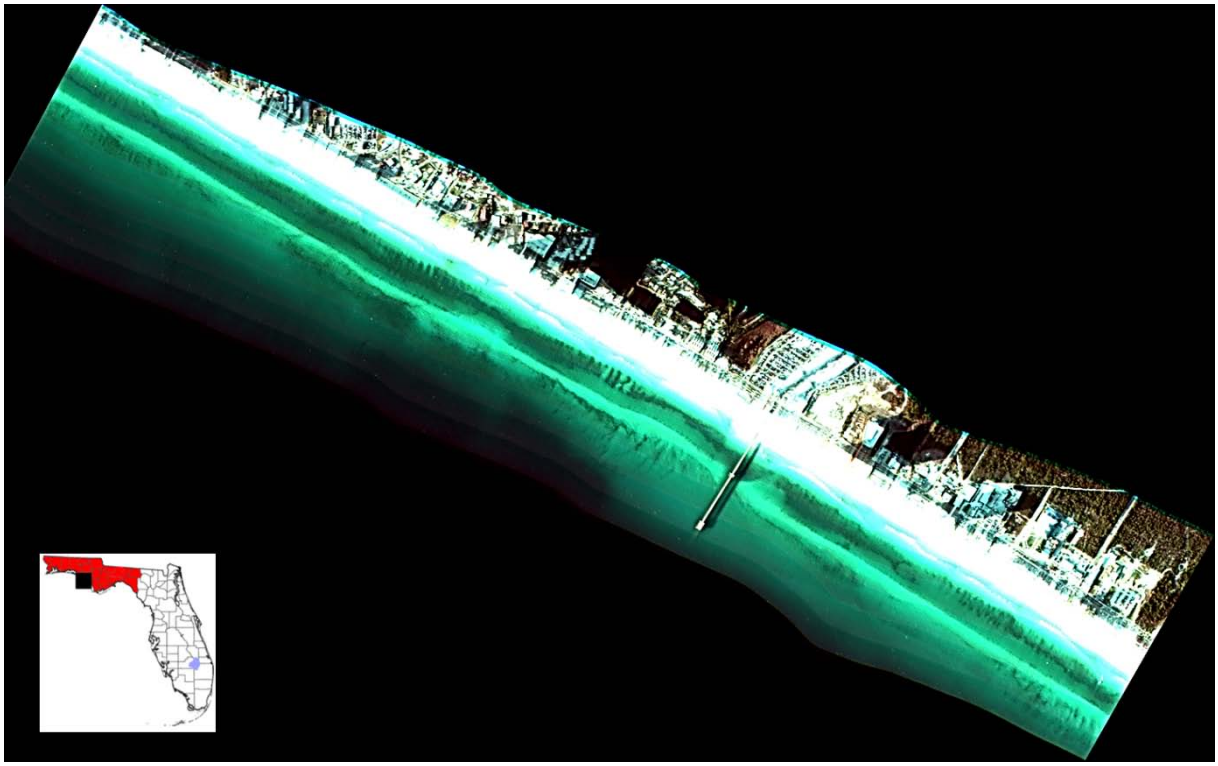

Figure 7. Hyperspectral reflectance flight line image near Panama City (Lullwater Beach Pier), Florida. (30°11'12.09"N 85°50'1.89"W). Flight line collected March 12, 2011 at 4,000 ft altitude during PM westbound flight along the Northern Gulf of Mexico. This HS image cube RGB display (684, 529, 488 nm bands) has been georeferenced, rectified and atmospherically corrected.

.

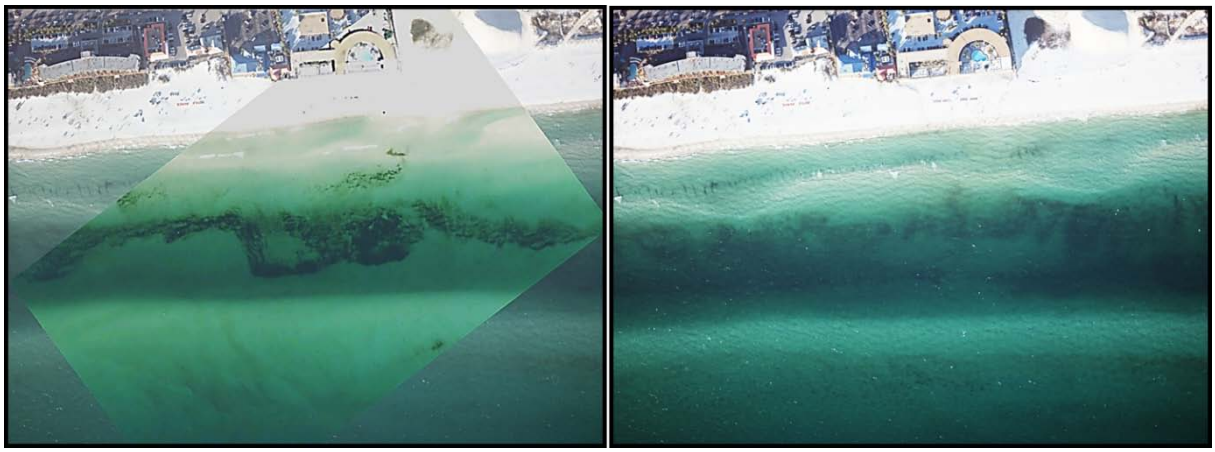

Figurer 8. Airborne scanned MS imagery along the Northern Gulf of Mexico during fall 2010 (left) and spring 2011 (right) indicating the change in indicated littoral zone weathered oil and thus the need for simultaneous multisensor[14] multispectral and hyperspectral image acquisition when utilizing the optimized spectral–spatial resolution enhancement methods to reduce fusion the difference between measured and synthetic signatures.

2.2. Description of the Data Fusion Methods

An brief overview of the approach to this optimized multi-sensor data fusion protocol methodology is shown in Figure 9. The first task in the image fusion process as mentioned above and shown below is image to image co-registration of the MS and HS imagery. The image to image georegistration process is important and can affect the final sharpened or synthetic data cube in terms of reducing blurring in the synthesized HS image fusion cube. The effects of poor image to image registration at this stage will result in a final product that has an out of focus view. Linear mapping of the MS and HSI imagery is then accomplished that essentially consists of a nearest neighborhood resampling. This is followed by definition of "*feature areas"*- areas of interest within which pixels are selected.

Random pixels are selected from these areas for use in optimized SVD model(s) development as shown in Equations 2 and 3. This stratified random sampling process (using different feature areas) provides pairs of pixels selected from the resampled multispectral channels and the co-registered channels from the MS imagery – for each channel in the HS data cube. The SVD results provide the estimated coefficients needed to generate a "*model image cube*" that is essentially predicted from using all of the multispectral channel data and the vector of SVD coefficients for each hyperspectral channel. As indicated, this research has shown the data fusion method used to select the pixels used in the analysis should be selected using user defined "*feature regions*" within the imagery in order to "*optimize"* the data fusion model building process. This stratified random sampling procedure of pixels to be used in the SVD analysis allows desired *image features* to be optimally modeled. The regions to include would be e.g. "suspected or known" surface or subsurface weathered oil areas in this application. Sensor saturated pixels need to be avoided in the pixel selection process in order to optimize the results. If this is approach is not followed, the resulting imagery will likely result in "saturated bleeding effects" in the sharpened imagery due to saturated pixels being used in the SVD model building process. The most critical steps are (1) precise image geo-registration, selection of regions of interest (avoid saturated channel pixels) and random selection of pixels from defined "feature areas" using a random number generator seed process. Models are optimized and selected based upon nonparametric K-S tests. Coefficients from the selected models can also be averaged for final K-S pixel tests before the SVD modeled HSI cube is synthesized using the spatial frequency filters. If SVD convergence does not occur with a valid K-S t-statistic, are resampled and/or feature areas redefined.

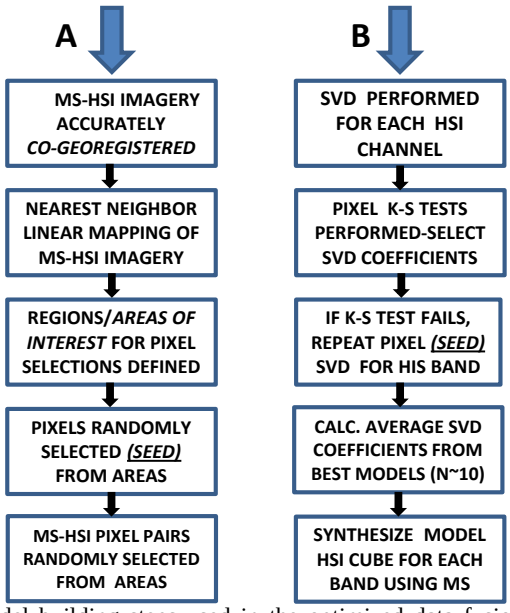

Figure 9. Overview of the SVD model building steps used in the optimized data fusion methodology. The above schematic indicates the general steps to generate the required SVD based modeled HS synthetic data cube. Every HSI channel model is optimized using the K-S test that is used to minimize the difference between the modeled and observed spectral signatures.

The SVD analyses uses pixels obtained from HSI imagery that has been (1) atmospherically corrected using a dark pixel subtraction technique[23,24], followed by (2) calculation of reflectance (using in scene spectrally known targets,

features or using spectral calibration targets. The MS imagery is based upon scanned TIFF imagery in digital counts obtained from the scanned 24 images shown in Figure 10. The SVD procedure can be described by:

$$H(h,i,j) = \sum_{k=1}^{B} a_k(h) M(k,i,j), \quad (1)$$

where:

$H(h,i,j)$ = predicted pixel value of the modeled hyperspectral image position i (rows), j (column) and band h (hyperspectral band),
B = the number of bands in the multispectral image,
$a_k(h)$ = the coefficient of the multispectral band for the hyperspectral band h to be estimated,
$M(k,i,j)$ = the multispectral pixel value at band k and position (i, j).

.

The above results in a simulated or "model" image where equation 1 yields:

$$H(h,i,j) = a_{red}(h) M(red,i,j) + a_{green}(h) M(green,i,j) + a_{blue}(h) M(blue,i,j), \quad (2)$$

where modeled high spatial resolution images have spectral signatures at each MS pixel for each h band (red, green, blue) from the HSI image cube. The SVD estimated vector of coefficients $a_k(h)$ are thus used to predict the model sharpened hyperspectral bands using the general linear model analysis. Thousands of pixels are randomly selected from the regions of interest or "feature areas" to perform the SVD. This results in a stratified random sample of (k,i,j) pixels used in the SVD. Because the multispectral and hyperspectral images have different spatial resolutions, their relative location is computed in both MS and HSI images using a linear mapping as depicted in Figure 2 as mentioned above.

Thus, pairs of pixels (MS images), and HSI spectrums are extracted at selected pixels. A modeled HSI data cube is synthesized using these SVD coefficients. The singular value decomposition method[25] produces the predictive matrix that contains the $a_k(h)$ coefficients for each channel. Essential to the process is linear mapping of the HSI imagery to the MS imagery using a nearest neighbor resampling algorithm depicted in Fig. 2.

The above process results in two different images that have been created: (1) a synthesized or modeled SVD based high spatial resolution HSI image cube using the $a_k(h)$ coefficients and (2) a georeferenced/coregistered mapped HSI image cube. An example is shown below of each image in the image process. After the SVD model cube is obtained, the discrete cosine transform (DCT) is applied in order place the modeled HSI image and the original HSI image in the spatial frequency domain. This procedure is accomplished using[26] a Type II DCT or:

$$F_l = \sum_{j=0}^{N-1} f_j \cos\left[\frac{\pi l}{N}\left(j + \frac{1}{2}\right)\right], \quad (3)$$

where:

F_l = the spatial-frequency-domain pixel at position l,
N = the total number of pixels to be transformed,
f_j = the spatial-domain pixel value in scaled non dimensional (digital counts or reflectance or radiance (W/m^2 str nm) at position j.

The DCT is a separable product[26] of two one-dimensional DCTs along each dimension as shown below:

$$\begin{aligned} F_{k,l} &= \sum_{i=0}^{M-1}\left(\sum_{j=0}^{N-1} f_{i,j} \cos\left[\frac{\pi l}{N}\left(j+\frac{1}{2}\right)\right]\right)\cos\left[\frac{\pi k}{M}\left(i+\frac{1}{2}\right)\right] \\ &= \sum_{i=0}^{M-1}\sum_{j=0}^{N-1} f_{i,j} \cos\left[\frac{\pi k}{M}\left(i+\frac{1}{2}\right)\right]\cos\left[\frac{\pi l}{N}\left(j+\frac{1}{2}\right)\right] \end{aligned}, \quad (4)$$

where:

$F_{k,j}$ = the spatial-frequency-domain pixel at position (k, l),
M ,N = the total number of rows and columns,
$f_{i,j}$ = spatial-domain pixel value at position (i, j).

Using this approach, $F_{k,j}$ can be computed in two steps by successive 1-D operations on rows and columns of an image[26]. An optimized two-dimensional DCT-II is applied to (1) each band of the original mapped, georeferenced and atmospherically corrected reflectance hyperspectral image cube and (2) to each band of the same modeled HSI image cube. After both of the image types have been converted to the spatial frequency domain, a 2D Butterworth filter is applied to each band in order to keep only the part of information that one desires to be included in the spectral-spatial sharpened image. A low-pass 2D Butterworth filter is applied to the mapped (low-spatial-resolution) HSI images and a high-pass filter is applied to the high-spatial-resolution SVD "model" HSI image (at each channel). The purpose of this procedure is to add the high (spatial) frequency content of the MS image to the HSI image cube. A 2 dimensional (2D) Butterworth filter is defined below where the high pass filter is equal to 1- B(x, y), and the low pass filter B(x, y) is given by:

$$B(x,y) = \frac{1}{1+\left(\frac{x}{cw}+\frac{y}{ch}\right)^{n}}, \quad \text{for } 1 \le x \le w, \text{ and } 1 \le y \le h, \tag{5}$$

where:

$B(x, y)$ = is the value of the filter at position (x, y),
c = the spatial-frequency of the image to pass (the cutoff),
w = the width of the image being filtered,
h = the height of the image being filtered,
n = the order of the filter.

The order of the filter (n) and the cut-off frequency (c) are "user variables" to be selected when running the software developed in our laboratory in parallelized C and *FORTRAN* programming languages. In essence, this filtering process keeps the high-spatial frequency in the SVD model HSI image cube and the low-spatial frequency in the original mapped georeferenced HSI image cube in order to "*synthesize*" a HSI image cube that has the spatial resolution of the multispectral image, but the spectral detail of the original hyperspectral signatures.

After both image types have been filtered, they are combined by addition (in the frequency domain). Resulting coefficients are just added in order to produce the sharpened image in the spatial-frequency domain. The high spatial frequencies of the final sharpened image have the spatial content from the original MS image. The remainder of the frequency domain contains the hyperspectral signature information at each pixel for each spectral channel or band.

The final spatial domain HSI image cube contains the spectral information in the form of the spectral signatures, but at a higher spatial resolution (~10 cm in this example). Note that the resulting synthesized imagery also contains the spatial detail originally found in the MS imagery, such as sharp edges or curvilinear features or "patch features" that originated in the high spatial resolution MS bands. To place the combined spatial frequency image "back" to the spatial domain, a two-dimensional *inverse* discrete cosine transform[26] (IDCT-II) is applied using:

$$f_{i,j} = \frac{2}{M}\frac{2}{N}C(i)C(j)\sum_{i=0}^{M-1}\sum_{j=0}^{N-1}F_{k,l}\cos\left[\frac{\pi k}{M}\left(i+\frac{1}{2}\right)\right]\cos\left[\frac{\pi l}{N}\left(j+\frac{1}{2}\right)\right], \tag{6}$$

where:

$F_{k,l}$ = the spatial-frequency-domain pixel at position (k, l),
M ,N = the total number of rows and columns,
$f_{i,j}$ = spatial-domain pixel value at position (i, j),

$$C(i) = \begin{cases} \frac{1}{2} & \text{if } i = 0 \\ 1 & \text{if } i > 0 \end{cases}, \quad \text{and} \quad C(j) = \begin{cases} \frac{1}{2} & \text{if } j = 0 \\ 1 & \text{if } j > 0 \end{cases}.$$

Similar to the 2D DCT-II, the 2D IDCT-II is expressed as a separable product of two 1D IDCT-II, one in each directions. A flowchart of the optimized data fusion method is shown in Figure 7 and Figure 9 as developed in this research. The schematic summarizes the algorithms (modified after Winter, Winter and Beaven[3]) using this optimized fusion methodology. This research has determined the procedure is somewhat insensitive to the 2D Butterworth filter order but *very sensitive to the cutoff frequency*. Thus, cutoff frequency is optimized for each set of images analyzed by minimizing the difference between the original selected hyperspectral pixel data used in the SVD analysis and the "synthesized" signatures (see Figure 9).

This optimization occurs for each HSI channel for pixels selected using the nonparametric K-S test procedure and is performed as a loop in the data fusion program as suggested in Figure 9 and previously reported[7]. Because the technique is sensitive to pixels selected, a split data validation technique is used where random sampling of pixels in user specified image areas are randomly selected and the SVD vector of coefficients are recomputed with high precision computing techniques.

The significant model coefficients (based on the k-S test p-statistic) SVD models are averaged. In essence, the K-S nonparametric test is used to select models (in a program loop) that minimize observed (mapped) and modeled or "synthetic" reflectance signature differences and then used again to select the *optimal cutoff frequency order*, where the K-S test is again used for selection the optimal cutoff and frequency for each hyperspectral channel.

3. RESULTS AND DISCUSSION

Figure 10 shows a resulting synthetic hyperspectral 3 band RGB image resulting from the resolution enhancement methodology using the MS and HS imagery shown in Figure 3 above. Figure 11 shows a sub-region in the shoreline imagery used to enhance the subsurface weathered oil spectral detection process. Figure 12 shows a similar region (see Figures 4, 5 for reference) and results of the optimized MS-HSI resolution enhancement or sharpening methods.

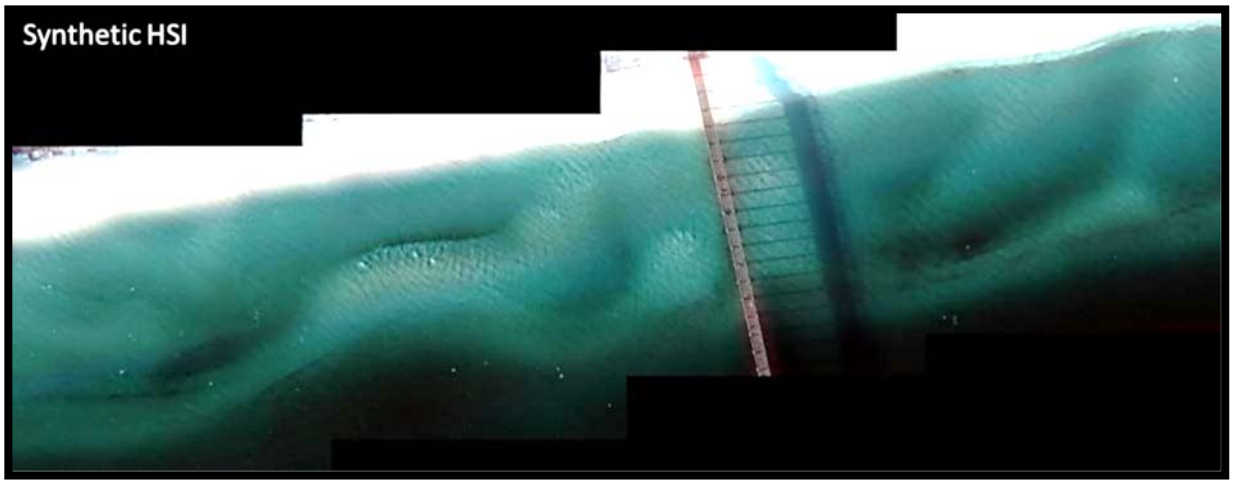

Figure 10 Synthetic hyperspectral image resulting from the optimized spectral –spatial resolution enhancement using the previously shown mosaic of MS and HS imagery used to perform spectral-spatial resolution enhancement. Imagery was collected March 12, 2011 along the Florida coastal waters in the Northern Gulf of Mexico at Navarre Beach Pier, 30°22'33.68"N 86051'46.76"W collected March 12, 2011 at 4,00 feet, westbound PM flight line.

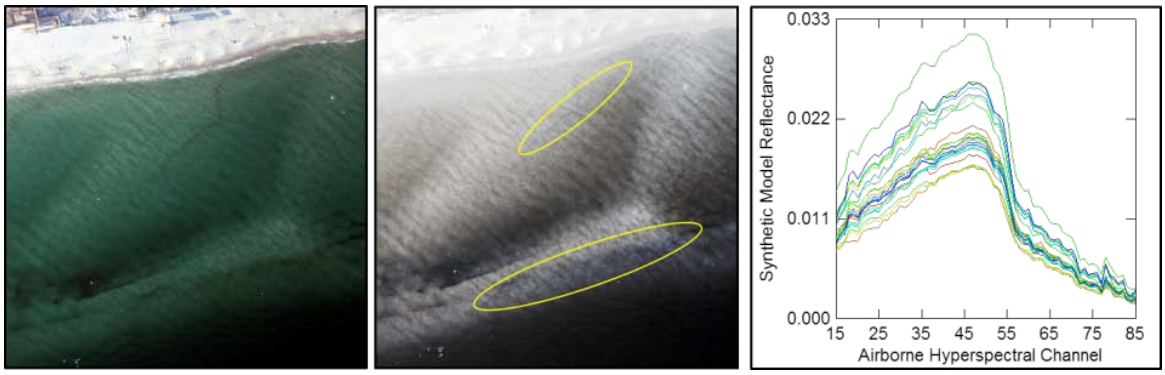

Figure 11. Scanned MS image (left) and the resolution enhanced HSI (RGB 3 band image) synthetic image (right) and associated reflectance spectra in the indicated areas. The resolution enhancement scene is from the March 12, 2011, PM westbound airborne flight line. Selected littoral zone synthetic spectra pixel size is ~10 cm at 4,000 feet. The flight line is in an area of reported littoral zone weathered subsurface oil near Navarre Beach, Florida along the northern Gulf of Mexico.

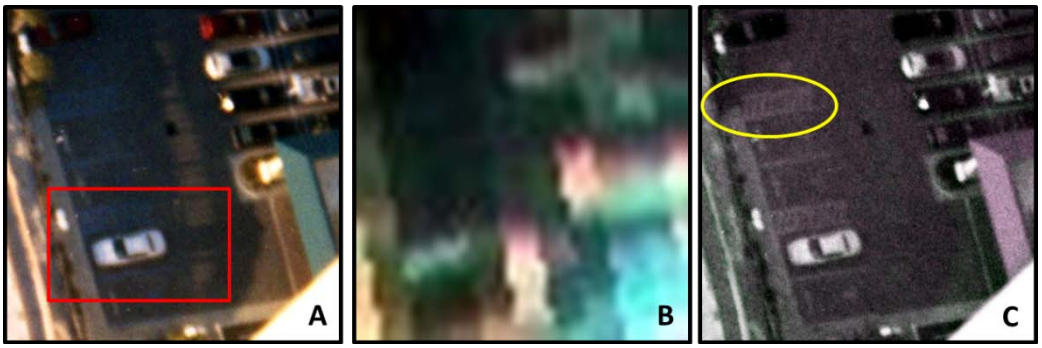

Figure 12. Example RGB displays of the use of ***feature areas*** (pixels in red box) used in the optimization of the spectral-spatial resolution enhancement SVD model building and use of wavelength dependent **cutoff optimization used to** improve resulting synthetic hyperspectral image cube channels. Image (a) is the MS image (512x512), image (b) is the HS image and image (c) is the resulting "optimized" synthetic hyperspectral cube image. Note the additional detail in the circled area in the resolution enhanced image and the removal of the shadow from a nearby building in image (c) in a littoral zone urban areas.

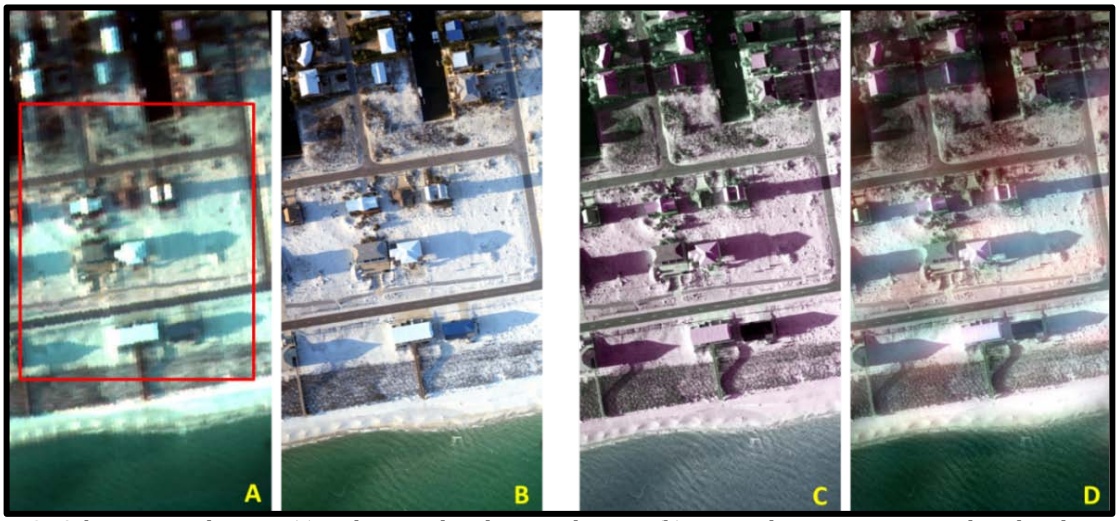

Figure 13. A hyperspectral image (a) and scanned multispectral image (b) are used to construct a single value decomposition modeled hyperspectral image cube (c) followed by application of the discrete cosine transform, the 2D Butterworth filter to the modeled and HS image cube, followed by the inverse discrete cosine filter that results in a resolution enhanced image cube (d). The above RGB 3 band image region were taken from Figure 3, and the outlined area in (a) represents the feature area were pixels were selected for SVD channel optimization. Cutoff and order optimization has been applied for each band.

The right image in Figure 14 is an example comparison between the measured and modeled HSI spectra are compared using the K-S test where the (1) SVD models and (2) cutoff frequency are "optimally selected". Final spectra are standardized before applying K-S tests and model comparisons. The optimization procedures are conducted in order to help insure spectral shape (adsorption and backscattering features) are preserved in the resolution enhanced reflectance spectra.

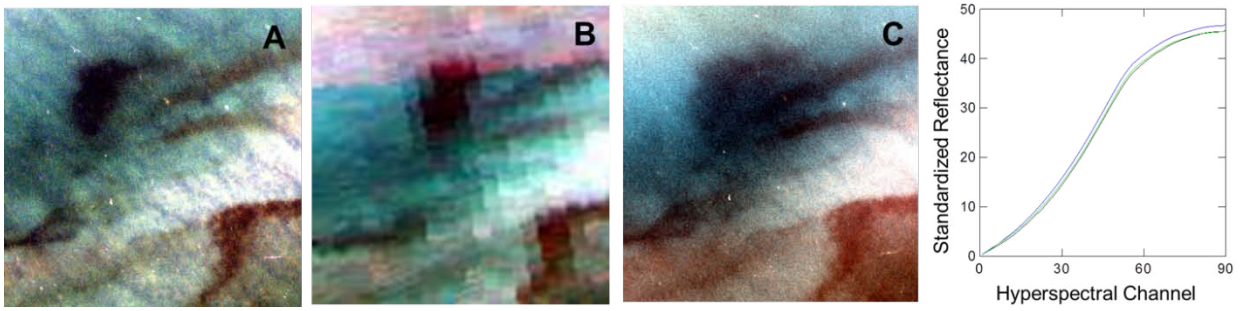

Figure 14. Example suspected subsurface oil patch in the littoral zone in a MS image (a), simultaneously collected HSI image (b) and the resulting same channels from the synthetic spectral-spatial enhanced HS image cube (c). The optimized SVD model coefficients, optimized cutoff and optimized order coefficients were used to obtain the result shown in (c) above. A characteristic randomly selected cumulative signature from the measured HS image (black) and the optimized model (blue) signature (blue) and the final sharpened spectral signature (green) is shown. The cumulative signature comparisons (right) are used to determine if the final spectral-spatial signatures are significantly different from the measured and modeled signatures using the nonparametric K-S test p-statistic in the channel by channel optimization methodology.

The optimized sharpened spectral signatures are also compared to measured signatures as shown in Figure 14 after optimizing the cutoff frequency and order as well the optimization procedure in the SVD model building process using nonparametric K-S p-statistic tests. In essence, once the optimal channel models are obtained using the SVD procedures, the optimum cutoff frequency and optimum order coefficients in the 2D Butterworth filter are determined using the difference between cumulative signature distribution plots as shown in Figure 14 (right). The resulting HS image cube contains pixel signatures representative of the original HS imagery but with spatial scales of the high spatial MS imagery. The method also works for multispectral sensor data from 2 different imaging systems with different spatial scales.

4. SUMMARY AND CONCLUSIONS

The purpose of this paper has been to describe the application of an optimized data fusion protocol[6] applied to airborne multispectral and hyperspectral imagery acquired simultaneously along the Northern Gulf of Mexico. The optimized approach is applied to imagery acquired as part of airborne remote sensing flights and missions following the Deepwater Horizon oil and gas spill along littoral zones that were reported to have evidence of subsurface weathered oil. The sensor calibration and image correction approaches and techniques used in the development and application of remote sensing imaging systems were described and form the basis of a multisensor data fusion approach. The high spatial and spectral resolution imagery shown in this paper is an example of technology for characterization of the water surface and subsurface features in aquatic systems and may be useful for continued or future weathered oil detection and subsurface feature detection in near coastal waters.

5. ACNOWLWDGEMENTS

The work presented in this paper has been supported in part by KB Science, and in part by funding from the Florida Institute of Oceanography - BP Corporation's Deepwater Horizon quick start research funding and the *airborne image acquisition* component of the 4D remote sensing project.

6. REFERENCES

[1] Esteban, J., Starr, A., Wiletts, R., Hannah, P., Bryanston-Cross, P., "A Review of Data Fusion Models and Architectures: Towards Engineering Guidelines", Neural Computing & Applications, 14(4), 273-281 (2005).

[2] Hardie, R., Eismann, M., Wilson, G., "MAP Estimation for Hyperspectral Image Resolution Enhancement Using an Auxiliary Sensor", In Proc IEEE Transactions on Image Processing, 13(9), 1174-1184 (2004).

[3] Winter, M., Winter, E., Beaven, S., "Resolution Enhancement of Hyperspectral Data Using Multispectral Imagery", SPIE Vol. 7473, pp. 74730F-1 to 12 (2009).

[4] Shettigara, K., "A Linear Transformation Technique for Spatial Enhancement of Multispectral Images Using a Higher Resolution Data Set", In Pro IEEE Geoscience and Remote Sensing Symposium, 4, pp. 2615-1618. (1989).

[5] Moeller, W., Wittman, T., Bertozzi, A., "A Variational Approach to Hyperspectral Image Fusion", SPIE Vol. 7334, pp. 73341-73341E-10, (2009)

[6] Bostater, C., Frystacky, H., Levaux, F., "Enhanced Data Fusion Protocol for Surface and Subsurface Imaging of Released Oil in Littoral Zones", In Proc ISOPE, ISBN 978-1-880653-94-4 pp. 808-814 (2012)

[7] Bostater, C., Frystacky, H., "Remote Sensing of Shorelines Using Data Fusion of Hyperspectral & Multispectral Imagery Acquired From Mobile and Fixed Platforms", SPIE Vol. 8390, pp. 8390261-17. (2012).

[8] Bostater, C., "Imaging Derivative Spectroscopy for Vegetation Dysfunction Assessments", SPIE Vol. 3499, pp. 277-285 (1998).

[9] Bostater, C., Coppin, G., Levaux, F., Jones, J., Frystacky, H., "Mobile Platform Pushbroom Motion Control. Image Corrections and Spectral Band Selection: Examples of Hyperspectral Imagery Using Low Flying Aircraft and Small Vessels in Coastal Littoral Areas", [In: Proceedings Robots for Risky Interventions and Environmental Surveillance-Maintenance (RISE-2011], International Advanced Robotic Program (IARP), Brussels, 1-19 pp. (2011).

[10] Hadjimitsis, D., Clayton, C., Retalis, A., "On the darkest pixel atmospheric correction algorithm: a revised procedure applied over satellite remotely sensed images intended for environmental applications", SPIE Vol. 5239, pp. 464-471 (2004).

[11] Siegel, D., Wang, M., Maritorena, S., Robinson, W., "Atmospheric Correction of satellite ocean color imagery: the black pixel assumption", Applied Optics, 39, pp. 3582-3591 (2000).

[12] Bostater, C., Coppin, G., Levaux, F., "Hyperspectral Remote Sensing Using Low Flying Aircraft and Small Vessels in Coastal Littoral Areas", [In: Remote Sensing – Advanced Techniques and Platforms], Escalante-Ramirez, B. (ed.), InTech Publishers, ISBN 978-953-51-0652-4, pp. 269-288 (2012).

[13] Hall, D., Llinas, J., "An Introduction to Multisensor Data Fusion", In Proc of the IEEE Vol. 85(1), pp. 6-23. (1977).

[14] Hall, D., Llinas, J. (eds.), [Handbook of Multisensor Data Fusion], CRC Press, Boca Raton, Florida, USA, ISBN 0-8493-2397-7, 568 pp. (2001)